Est. 1984

ORIENTAL JOURNAL OF CHEMISTRY
An International Open Access, Peer Reviewed Research Journal

www.orientjchem.org

ISSN: 0970-020 X
CODEN: OJCHEG
2022, Vol. 38, No.(5):
Pg. 1276-1283

Corrosion Inhibition Activity of Isolated Flavonoid from *Andrographis echioides* Leaves

S. DURGADEVI[1]*, A. LEEMA ROSE[2], S. VIDHYA[3], F. JANEETA PRIYA[4] and P. LYDIA FESTUS KANMANI[5]

*[1,2,3,4,5]Department of Chemistry, Holy Cross College (Autonomous), Affiliated to Bharathidasan University, Trichy-2, India.
*Corresponding author E-mail: saiganessh2014@gmail.com

http://dx.doi.org/10.13005/ojc/380525

(Received: July 03, 2022; Accepted: September 16, 2022)

ABSTRACT

Andrographis echioides leaves were used to isolate a flavonoid (medicarpin) that inhibited mild steel corrosion in 1M HCl. Preliminary phytochemical analysis revealed that the A.E leaves were rich in flavonoids. Following a room temperature extraction with methanol, the constituents were fractionated using a soxhlet apparatus. Chromatographic techniques were used to isolate the constituents from the leaves of *Andrographis echioides*. Flavonoid compounds were characterized using spectral studies. Weight loss and corrosion studies were investigated the inhibition activity of an isolated flavonoid (medicarpin). The inhibition efficiency of isolated flavonoid was highest (85.78 percent) at 800ppm concentration, according to weight loss and electrochemical measurements. The influence of temperature on the corrosion activities of base metal was calculated in the temperature range 293-303K. The inhibitory activity increases with rising inhibitor concentration but decreases with rising temperature. The activation and free energies for the inhibition response sustain the method of physisorption. The adsorption of isolated flavonoid on the base metal is an endothermic process and it follows the Langmuir adsorption isotherm. The potentiostatic study illustrates that isolated flavonoid is a mixed type inhibitor. Surface Morphology Examination by SEM and EDAX to reveals the adherence of isolated flavonoid on the mild steel surface.

Keywords: *Andrographis echioides*, Flavonoid, Corrosion studies, SEM, EDAX.

INTRODUCTION

Corrosion of metals and their alloys caused mechanical failure of equipment due to acid and alkaline exposure. Corrosion inhibitors are typically included in trace levels to slow metal corrosion[1]. Corrosion damage can be avoided through a variety of methods, including material improvements, fluid blending, process control, and chemical inhibition. Among these methods, the use of corrosion inhibitors is the most effective in preventing metal surface destruction or degradation in corrosive media. Corrosion inhibitors are the most cost-effective and practical method of reducing corrosive attack on metals. The majority of corrosion inhibitors are toxic, non-biodegradable, and costly[2]. This prompted

the development and use of environmentally friendly corrosion inhibitors. Plant extracts were environmentally friendly, readily available, and cost effective[3], and they outperformed synthetic corrosion inhibitors. Plant extracts have been used in corrosive environments to prevent corrosion[1,4-13].

The several sustainable and environment corrosion inhibitors have recently become available. Anticorrosion properties of flavonoid separated from Nypa Fructicans Wurmb leaf[14], Anacyclus pyrethrum L. stem[15], and Mentha Pulegium leaf extract[16] have been successfully reported. The observed results revealed that all of the previous mentioned plants have excellent anticorrosion properties and are, most importantly, efficient and environmentally. This survey demonstrates the potential of an isolated flavonoid from Andrographis echioides leaf extract acts as a mild steel corrosion protection in hydrochloric acid solution.

Fig. 1. *Andrographis echioides* plant

EXPERIMENTAL METHODS

Preparation of the Sample

The sample was made from a readily obtainable manufacturing Fe-C steel with low carbon content and an element composition of 0.026 percent S, 0.06 percent P, 0.4 percent Mn, and 0.1 percent C, as well as reminder Fe. The samples were mechanically polished after being degreased with various types of emery paper, washed in double filtered water, and thoroughly cleaned with acetone before being kept in humidity-free desiccators for later use.

Preparation of inhibitor solution

1 g of confined flavonoid is concentrated to 1000 parts per million in 1000 mL solutions (ppm). The concentration utilized in the study ranged from 100 to 900 parts per million.

Measurements of weight reduction

The Shimadzu ATP-224 model digital weighing balance was used to monitor weight loss, with a readability of 0.1 mg in the 210 g. The sample was submerged in a 100 mL acid solution with and without isolated flavonoid extracts using hooks. The sample were removed, cleaned in deionized water, dried, and weighed again.

Altering Current impedance measurements

Electrochemical readings were executed using AC signals with maximum amplitudes of 10mV at constant current capacity in the occurrence range of 10MHZ to 1HZ. The electrochemical reactions response (R_{ct}) values were deliberated based on the comparing the impedance between small and elevated frequencies. The transformed of the two deposit values are derived from the frequency (f) at which the unreal factor of the internal resistance is greatest, and the equivalent circuit of the double layer (C_{dl}) is calculated[17].

Potentiodynamic polarization study

CHI electrochemical impedance analyzer model 660A has been used for potentiodynamic polarization experiments. After acquiring the impedance spectrum, the current potential graphs were noted all at once by modifying the electrolytic potential routinely captured from the OCP value at a test rate of 5mV s^{-1}. For the studied systems, the Tafel strands extrapolation technique was used to detect icorr and E_{corr} values. Because the acquired polarization curves contained nonlinearity, the correlating Tafel slopes (ba and bc) were determined using a computer least square analysis as a gradient of the points following corrosion capacity I by 50 mill volts. All electrolytic experiments were completed in stagnated, oxygenated solutions at 30°C.

Scanning electron microscopy

The low carbon steel specimens were removed by washing with double filtered water, dried, and surface evaluated after three hours in the appearance and nonappearance of inhibitor. The carbon steel layer was SEM measured using a CAREL ZEISS EVO-18- High Resolution Scanning Electron Microscope at St. Joseph's College in Trichy.

Energy dispersive X-ray analysis

EDAX is a method for elemental analysis or chemical identification of a sample. The samples

were delayed in a solution with inside or use plastic grips for 3 hours. After 3 h, the specimen was removed, and the metal specimen was sent to National College, Trichy, for EDX analysis.

RESULT AND DISCUSSION

Mass loss method

At 30°C, Corrosion potential of thin metal in 1M Hydrochloric acid was investigated using loss of weight measurements in the absence and presence of isolated flavonoid from *A. echioides* leaves, and the proportion of inhibitory activity was detected. Table 1 depicts the corrosion rate (mpy) and removal efficiency with increasing inhibitor concentration (in ppm). According to the information, the corrosion rate diminishes noticeably with hiking inhibitor concentration, whereas corrosion inhibition increases with increasing inhibitor concentration[18]. At 3 h immersion in 1M Hydrochloric acid, the extreme efficiency of inhibitory activity of isolated flavonoid at 800ppm concentration was found to be 85.78 percent. This is because of adsorbent inhibition with the base metal surface rises with accumulation of inhibitor.

Table 1: Represents Corrosion rates of isolated Flavonoid

Sr. No	Isolated flavonoid (ppm)	Corrosion rate(mpy)	Surfacecoverage(θ)	PercentageInhibition(%)
1	Blank	11.2780	-	
2	100	7.1929	0.37	37.33
3	200	5.9379	0.48	48.27
4	300	5.1115	0.55	55.47
5	400	4.5453	0.60	60.40
6	500	4.1320	0.64	64.00
7	600	3.4740	0.69	69.88
8	700	3.0000	0.73	73.86
9	800	1.6319	0.85	85.78
10	900	1.9742	0.82	82.80

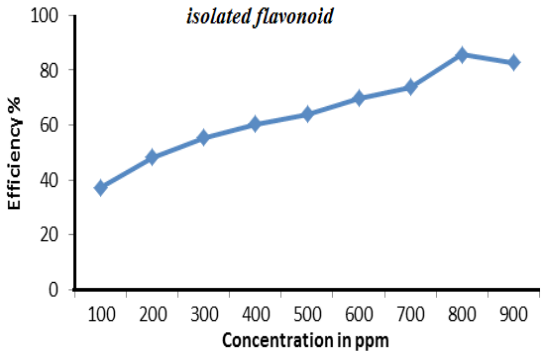

Fig. 2. Inhibition efficiency of isolated flavonoid extract at various concentration

Influence of temperature

Figure 3 depicts the temperature dependence of the inhibitor's percentage inhibition at varying temperatures. The information display that the inhibition efficiency decreases as the temperature rises. The diminish in inhibition tendency with enlarging temperature specifies dissociation of the inhibitor from the surface of the base metal. This is owing to a faster rate of disintegration of mild steel and partial decomposition of the inhibition from the base metal substrate as temperature rises.[19,20]

Table 2: Mention that temperature of the isolated flavonoid

Sr. No	Temperature(K)	Corrosion rate(Blank)	Corrosion rate(inhibitor)	Surface coverage(θ)	% I.E
1	303	11.4780	1.6319	0.85	85.78
2	313	22.9101	7.5755	0.66	66.93
3	323	31.4497	16.2528	0.48	48.32
4	333	44.8713	31.8629	0.28	28.99

Kinetic and thermodynamic corrosion rate parameters

The corrosion rate of a chemical reaction is temperature dependent, and this temperature dependence corrosion rate can be demonstrated using the Arrhenius and transition state equations[21].

$$Log(C_R) = -\frac{Ea}{2.303\,RT} + log\lambda \quad (1)$$

$$C_R = \frac{RT}{Nh}\exp\left(\frac{\Delta S^*}{R}\right)\exp\left(\frac{-\Delta H^{\neq}}{RT}\right) \quad (2)$$

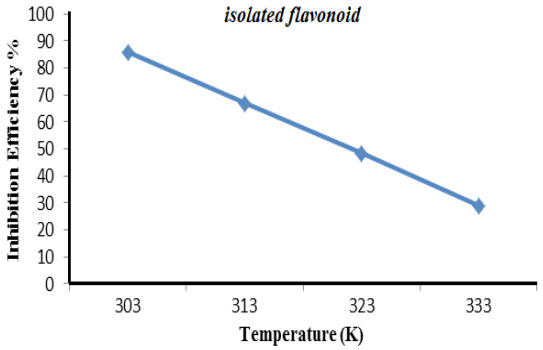

Fig. 3. Inhibitory activity of isolated flavonoid at various temperatures

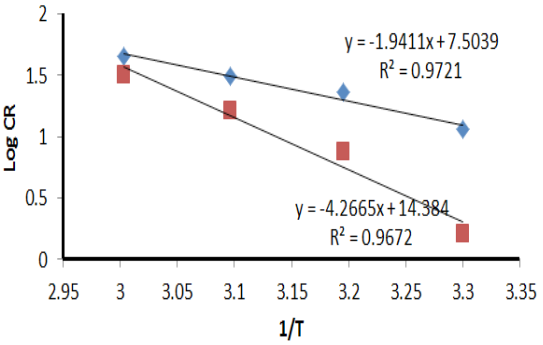

Fig. 4. Plots for corrosion of mild steel in 1M HCl and isolated flavonoid

All linear regression correlation value is close to one. Table 4 depicts that E_a values are higher in the appearance of the inhibitor in comparison to the nonappearance of the inhibitor. The increase in E_a might be accredited to physical activation[22]. The increase in E_a value in the presence of inhibitor may be attributed to increased double layer thickness, which slows the corrosion process[23].

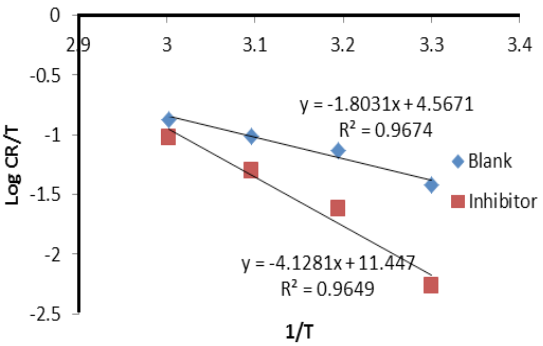

Fig. 5. log CR/T versus 1/T

From the graph, we conclude that straight lines of the ΔH* and ΔS*. Table 3 suggests that the value of ΔH* for dissolution of low carbon steel in 1M HCl in presence of isolated flavonoid is significantly greater (79.04kJ/mol^{-1}) than in the absence of isolated flavonoid (34.52 kJ/mol^{-1}). The sign of positive and significant level of H* reflected the heat absorbed in the mild steel dissolution system, implying that thin metal disintegration is difficult in the presence of isolated flavonoid[24]. The transition toward positive entropies (S*) suggests that the complex activation within the rate-determining sequence represents dissociation rather than affiliation, implying that disordering will increase as reactants are transferred to the complex activation[25].

The modification of ΔH* and ΔS* with inhibitor concentration indicates that the procedure is enthalpic and thermodynamically controlled[26].

Table 3: Kinetic and thermodynamic criteria of isolated flavonoid

	Ea(kJmol^{-1})	ΔH*(kJmol^{-1})	ΔS*(kJmol^{-1})
Blank	91.902	34.52	0.077
Inhibitor	242.74	79.04	0.209

Adsorption parameter

The graph was created by fitting the fraction of the surface covered to Langmuir's isotherm, which implies a solid surface has a predetermined percentage of adsorption sites with one adsorbed species at each site[27]. The weight loss method value is entered into the Langmuir adsorption isotherm equation, and a graph of C/θ versus C is plotted.

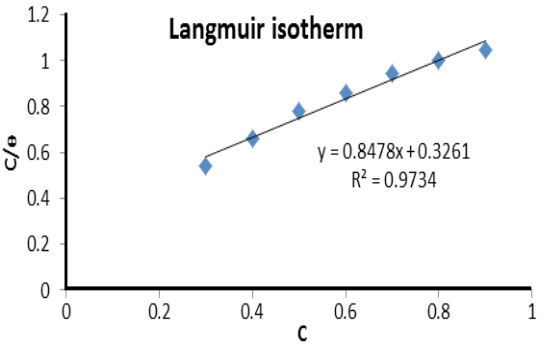

Fig. 6. Langmuir adsorption plot

Table 4: Langmuir adsorption of isolated flavonoid in 1M HCl on the mild steel

Inhibitor	Intercept	K_{ads}	R^2	ΔG_{ads}^0(kJmol^{-1})
Isolated flavonoid	0.3261	3.0665	0.9734	-12.944

The R^2 is 0.97, and the gradient is related to 1[28], representing that the Langmuir isotherm is strongly adhered to Fig. 5. In general, $\Delta G°_{ads}$ values less than 20 kJ mol^{-1} indicate physisorption, while values greater than 40 $kJmol^{-1}$ indicate chemisorptions[29]. In Table 4, the fact that $\Delta G°_{ads}$ is negative indicates to be spontaneous. Physical adsorption is indicated by the calculated $\Delta G°_{ads}$ is -12.994kJ mol^{-1}, which is less than $-20kJmol^{-1}$ [30].

Potentiodynamic polarization studies

Figure 7a, b depicts the electrochemical polarization behaviour of base metal in 1M HCl in the absence and occurrence of isolated flavonoid as a Tafel plot. The reduction in corrosion potential after the additament of the inhibitor signifies that the extract is used as an inhibitor and diminishes base metal corrosion in acidic condition. The raise in the value of β_a is substantially more than that of β_c. The decrease in the E_{corr} denotes that the inhibitor primarily functions as an anodic inhibitor[31].

Electrochemical impedance parameter

Figure 8a, b illustration the impedance behaviour of thin metal in 1M HCl in the appearance and non appearance of isolated flavonoid as a Nyquist plot, and Table 6 shows EIS parameters that are generated from the Nyquist plot. The increased R_{ct} and decreased C_{dl} values obtained from impedance studies support a compound's good performance as an inhibitor in destructive medium. This behaviour indicates that the obtained film provides a barrier to the corrosion process, which demonstrates the film's formation[32].

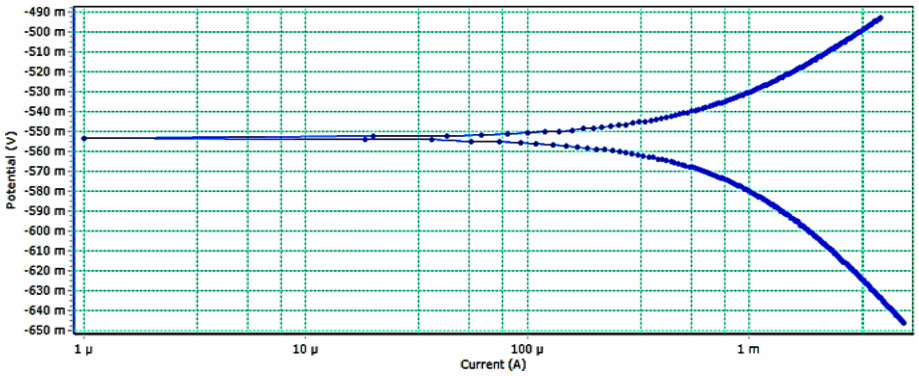

Fig. 7a. Tafel polarization curves without isolated flavonoid

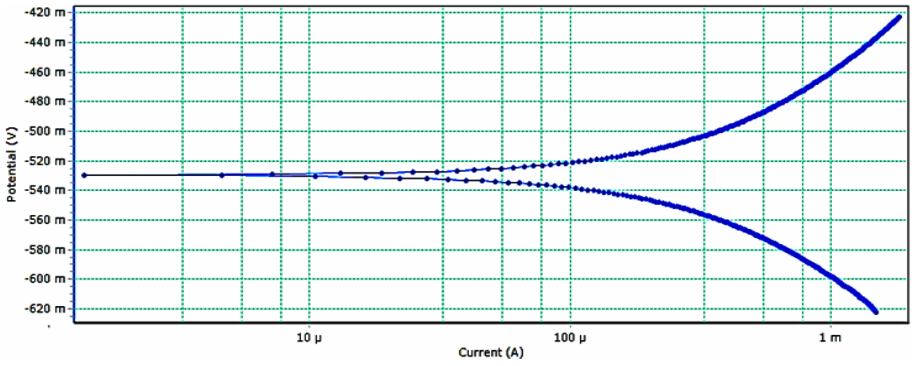

Fig. 7b. Tafel polarization curves with isolated flavonoid

Table 5: Potentiodynamic and linear polarization criteria of isolated flavonoid

System	E_{corr} mV/SCE	I_{corr} µA/cm^2	β_a mV/dec	β_c mV/dec	C_{orr}.rateMm/y
Blank	-553.4	857.7	90.123	119.159	392.0
Inhibitor	-529.7	370.9	144.827	141.932	169.5

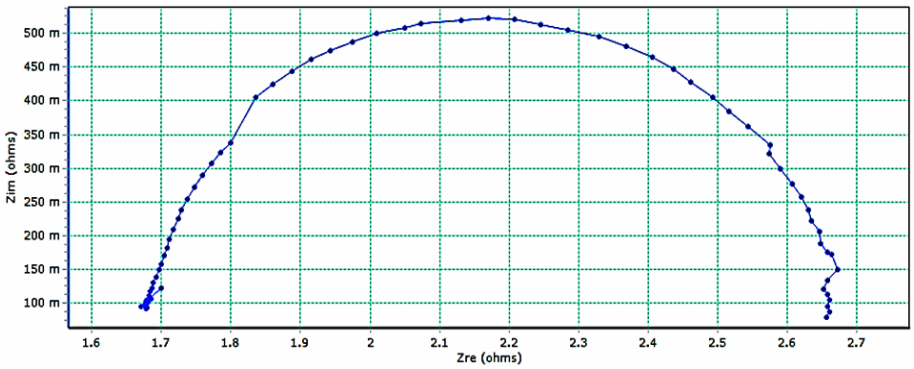

Fig. 8a. Nyquist plot in absence of isolated flavonoid

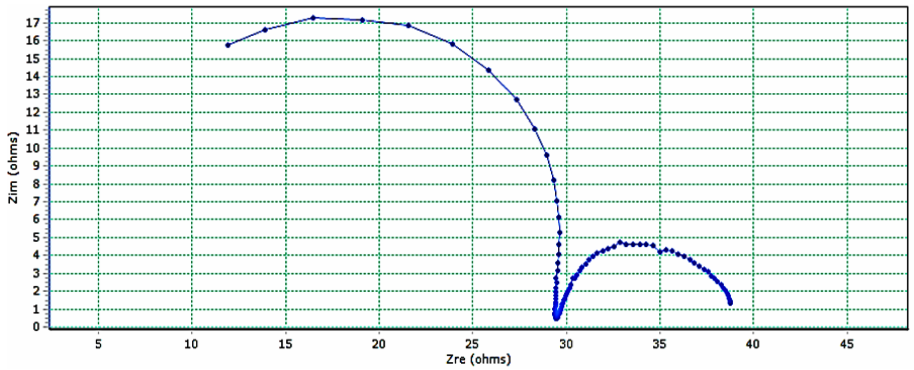

Fig. 8b. Nyquist plot in presence of isolated flavonoid

Table 6: The electrochemical impedance values of isolated flavonoid

System	$R_s\Omega$	$R_{ct}\Omega m$	C_{dl} Fm
Blank	1.67	0.99207	0.0739
Inhibitor	5.1	23.374	3.79×10^{-4}

SEM analysis

Inhibitor molecules contact with the base metal was studied using Surface morphology. Surface morphology of plain base metal, base metal is immersed in 1M HCl, and steel dipped in 1M HCl with isolated flavonoid were shown in Fig. 9. According to the SEM images, the thin metal specimen dipped in the inhibitory solution is in good state, with a plain surface, whereas the metal surface dipped in the acidic medium is hardness and appears to be full of cracks and holes[33]. It validates isolated flavonoid forms a protective barrier on the sample, lowering the corrosion rate[34].

EDAX analysis

The EDAX method was used to determine the surface composition of the base metal sample in 1M HCl solution in the lack and appearance of the inhibitor. The EDX spectrum of uncontrolled metal samples and inhibited thin metal samples are shown in the Figure (A) & (B).

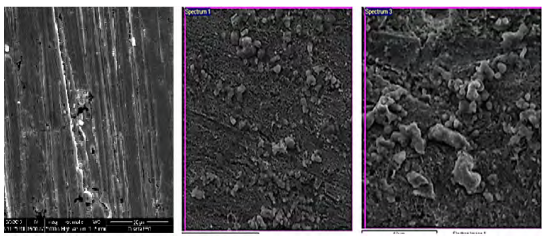

Fig. 9. SEM micrograph of (a) plain metal (b) metal in acid, (c) metal in isolated flavonoid (800ppm)

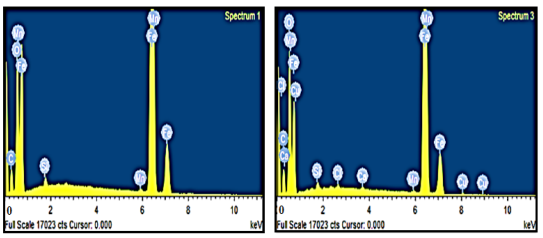

Fig. 10. EDAX spectra of (A) mild steel specimen and (B) presence of isolated flavonoid

This graph depicts the atomic content of several elements measured by EDX in uninhibited and inhibited base metal surfaces. The presence of base metal components can be seen in the EDX spectra. In this table, the oxygen percentage in isolated flavonoid is higher, indicating that it may be absorbed on the specimen's surface.

Table 7: Shows that atomic content of elements

Mild steel	Fe	C	O	Si	Cl	Ca	Mn	Cu
Blank	37.46	26.06	35.69	0.58	-	-	0.20	-
Inhibitor	33.25	26.24	39.43	0.45	0.20	0.12	0.18	0.15

CONCLUSION

Isolated flavonoid is a good corrosion inhibitor for mild steel corrosion in 1M Hydrochloric acid solution. At 800ppm, the maximum efficiency was found to be 85.78 percent. The Langmuir isotherm was followed by the adsorption of isolated flavonoid extract on a mild steel surface. Potentiodynamic studies show that isolated flavonoid extract acts as a mixed type inhibitor, primarily as an anodic inhibitor. EIS measurements revealed that higher the inhibitor concentration raised the resistance of the base metal electrode while diminish its inductance. The presence of negative ΔG values designates that the adsorption of isolated flavonoid extract on base metal to be spontaneous. Because Ea gradually increases to inhibitor concentration, the efficiency barrier for the corrosion interaction increases as well. The surface morphology and defensive film of the thin layer on base metal are investigated using SEM analysis and EDAX spectra. Mass loss and electrochemical results shows that A.echioides leaves extract isolated flavonoid acts as a good inhibitor.

ACKNOWLEDGEMENT

Thanks for Holy Cross College (Autonomous), Trichy for providing lab and library facilities.

REFERENCES

1. Ebenso, E. E.; Eddy, N.O.; and Odiongenyi, A.O.; *African Journal of Pure and Applied Chemistry.*, **2008**, *11*, 107-115.
2. Abiola,O.K.; James, A.O.; *Corrosion Science.*, **2010**, *52*, 661-664.
3. Abiola, O. K.; Otaigbe, J. O. E.; Kio. O. A.; *Corrosion Science.*, **2009**, *51*, 1879-1881.
4. Abiola O. K.; Oforka N. C.; Ebenso E. E.; Nwinuka N. M.; *Anti-Corrosion Methods & Materials.*, **2007**, *54*, 219-224.
5. Oguzie, E. E.; *Portugaliae Electrochimica Acta.*, **2008**, *26*(3), 303-314.
6. James, A.O.; Etela, A. O.; *Journal of Pure & Applied Chemistry.*, **2008**, *3*(3), 141-145.
7. Kalada, H. and James, A.O., *Journal of Emerging Trends in Engineering and Applied Sciences.*, **2014**, *5*(1), 24-29.
8. Sribharathy, V.; Rajendran, S.; Hindawi Publishing Corporation, ISRN Corrosion, **2013**, 1-7.
9. Fouda, A. S.; Tawfik, H.; Badr, A. H.; *Advances in Mat. and Corrosion.,* **2012**, *1*, 1-21.
10. Orubite-Okorosaye, K.; Jack, I.R.; Ochei, M.; Akaranta,O.; *J. Applied Science and Env. Management.*m, **2007**, *11*(2), 27-31.
11. Omotosho, O. A.; Ajayi, O. O.; Ajanaku, K. O.; Ifepe, V. O.; *J. Mat.* and *Env. Science.*, **2012**, *3*(1) 66-75.
12. Vimala, J. R.; Leema, A. R.; Raja, S., *Inter.J. of Chem Tech Research.*, **2011**, *3*(4), 1791-1801.
13. Avwiri, G. O.; and Osarolube, E.; *Scientia Africana.*, **2010**, *9*(2), 51-58.
14. Nwaugbo Chinenye Michael, James Abosede Olubunmi, *Sci. J. Chem.*, **2014**, *2*(4), 27-32.
15. Selles C.; B. Omar, T. Boufeldja.; L. Larabi.; Y. Harek.; *J. Mater. Environ. Sci.*, **2012**, *3*, 206-219.
16. Khadraoui A.; A. Khelifa.; K. Hachama.; H. Boutoumi.; B. Hammouti., *Res. Che. Inter.*, **2015**, *41*, 7973-7980.
172. Hsu, C. S.; Mansfeld,P.; *Corrosion.*, **2001**, *57*, 747.
18. Li, X.H.; Mu, G.N.; *Applied Surface Science.*, **2005**, *252*, 1254.
19. Ahamed I, Prasad. R and Quraishi M.A, *Corrosion Science.*, **2010**, *52*, 3033.
20. Sudheer, Quraishi, M.A.; *Corrosion Science.*, **2013**, *70*, 161
21. Ahamed,I.; Prasad, R.; Quraishi, M. A.; *Corrosion Science.*, **2010**, *52*, 1472-1481.
22. Mernari B.; El Kadi L.; Kertit S., *Bull Electrochem.*, **2001**, *17*(3), 115.

23. Oguzie EE., *Corrosion Sci*, **2008**, *50*(11), 2993.
24. Guan, N. M.; Xueming, L.; Fi, L.; *Mater.Chem. Phys.*, **2004**, *86*, 59-68.
25. Quraishi, M. A.; Singh, A.; Singh, V. K.; Yadav D. K.; Singh, A. K.; *Mater. Chem. Phys.*, **2010**, *122*, 144.
26. Granese, S.L.; Rosales, B.M.; 10th *International congress on metallic corrosion*, III, Madras, India., **1987**, 2733.
27. Yuce AO.; Solmazb R.; Kardas G.; *Mater Chem Phys.*, **2012**, *131*, 615–620.
28. Bilgic S.; Sahin M.; *Mater Chem Phy.*, **2001**, *70*, 290.
29. Ahamad I.; Prasad R.; Quraishi MA., *Corrosion Sci.*, **2010**, *52*, 1472.
30. Fekry AM.; Mohamed RR., *Electrochim Acta.*, **2010**, *55*, 1933.
31. Sandhya Rani M.; Rao S.; Pippalla KM., *JPRHC.,* **2009,** *1*(1), 97.
32. Prabhu RA.; Venkatesha TV.; Shanbhag AV.; Kulkarni GM.; Kalkhambkar RG., *Corrosion Sci.,* **2008**, *50*, 3356–3362.
33. Mitali Konwar.; G D Baruah.; *Archives of Applied Science Research.*, **2011**, *3*(1), 214-221.
34. Vidhya S.; Leema Rose A and Janeeta Priya F, *Asian Journal of Chemistry.*, **2019**, *31*(10), 21964.